

A High-Gain and Broadband 1×8 Hexagonal Antenna Array for 28 GHz 5G Applications

Ghizlane Mounir

ERSC Research Team, Mohammadia School of Engineering, Mohammed V University in Rabat, Morocco

mounir.ghizlane@research.emi.ac.ma

Jamal El Abbadi

ERSC Research Team, Mohammadia School of Engineering, Mohammed V University in Rabat, Morocco

elabbadi@emi.ac.ma (corresponding author)

Received: 1 December 2025 | Revised: 15 January 2026 and 9 February 2026 | Accepted: 19 February 2026

Licensed under a CC-BY 4.0 license | Copyright (c) by the authors | DOI: <https://doi.org/10.48084/etasr.16641>

ABSTRACT

Millimeter-wave (mmWave) fifth-generation (5G) communication systems operating at 28 GHz experience significant propagation losses, which necessitate the use of compact, high-gain, and wideband antenna arrays. In this paper, a novel 1×8 hexagonal microstrip antenna array is proposed for 5G mmWave applications. The array is designed on a Rogers RT5880 substrate with a relative permittivity of 2.2, a loss tangent of 0.0009, and a thickness of 0.45 mm. By employing a hexagonal radiating geometry and a T-junction corporate feeding network, the proposed array achieves improved current distribution and efficient aperture utilization. Simulation results demonstrate that the proposed antenna array attains a high realized gain of approximately 14.32 dB, surpassing that of several previously reported microstrip-based arrays, along with a wide impedance bandwidth of 1.84 GHz. Good impedance matching and stable radiation characteristics are maintained across the operating band. Compared with conventional patch-based arrays reported in the literature, the proposed design offers enhanced gain and bandwidth performance while preserving a compact structure. These features make the proposed hexagonal antenna array a promising candidate for 5G mmWave systems requiring high directivity, broadband operation, and compact implementation.

Keywords-5G mmWave; 28 GHz; hexagonal microstrip antenna; antenna array; high-gain; beamforming; RT5880

I. INTRODUCTION

Fifth-generation (5G) wireless communication represents a major technological leap, enabling Ultra-Reliable Low-Latency Communications (URLLC), enhanced Mobile Broadband (eMBB), and massive Machine-Type Communications (mMTC) [1-3], supporting emerging applications such as the Internet of Things (IoT), smart cities, autonomous vehicles, and high-data-rate multimedia services. To satisfy the stringent performance requirements of these applications, the exploitation of millimeter-wave (mmWave) frequency bands has become fundamental, particularly around the 28 GHz band, which offers a favorable compromise between available bandwidth and propagation characteristics [4-7]. Despite these advantages, mmWave signals suffer from severe free-space path loss, atmospheric attenuation, and limited diffraction at high frequencies [8, 9], necessitating advanced antenna systems with high gain, directional radiation patterns, wide impedance bandwidth, and compact geometries suitable for integration into modern wireless terminals and base stations; consequently, antenna array configurations have become essential

components of mmWave 5G communication systems [10]. Microstrip patch antennas are widely regarded as strong candidates due to their low profile, lightweight structure, ease of fabrication, and compatibility with planar integrated circuits [11-15], but conventional single-element designs exhibit limited gain and narrow impedance bandwidth, restricting their effectiveness at high frequencies [16]. To address these limitations, numerous studies have investigated antenna arrays, optimized patch geometries, and advanced feeding networks to enhance radiation performance [17-20], with most reported 28 GHz designs relying on conventional rectangular or circular patches and relatively limited array configurations. From an electromagnetic perspective, the hexagonal patch geometry provides several advantages over circular, square, or rectangular patches; its six-sided symmetry promotes uniform surface current distribution and smoother current flow along edges, improving impedance matching, operational bandwidth, radiation efficiency, and gain while maintaining a compact footprint suitable for mmWave 5G devices. Motivated by these benefits, this paper proposes a novel 1×8 hexagonal microstrip

antenna array operating at 28 GHz, employing a corporate T-junction feeding network to ensure uniform power distribution and phase coherence among the array elements. Simulation results demonstrate a high gain of approximately 14.32 dB, a wide impedance bandwidth of 1.84 GHz, and a highly directive radiation pattern, making the proposed array a promising candidate for next-generation 5G mmWave communication systems.

II. ANTENNA CONFIGURATION

A. Geometry of Hexagonal Patch Antenna

The proposed hexagonal microstrip antenna element (Figure 1) is designed on a Rogers RT5880 dielectric substrate with a thickness of 0.45 mm, a loss tangent of 0.0009, and a relative permittivity of $\epsilon_r = 2.2$. To ensure proper impedance matching, a quarter-wavelength transformer is integrated between the feed line and the patch. The initial design parameters were determined using classical transmission line theory [21], and the optimized dimensions are summarized in Table I.

TABLE I. OPTIMIZED GEOMETRICAL DIMENSIONS OF THE HEXAGONAL ANTENNA ELEMENT

Parameter	Value (mm)
Wa	1.72
Wq	0.15
Lq	2.5
Wf	1.55
Lf	2.05
W	11.44
L	11.99

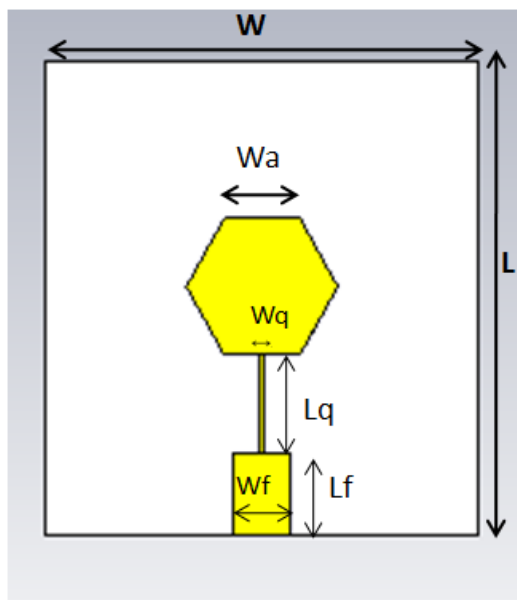


Fig. 1. Geometry of the hexagonal antenna element.

The hexagonal patch geometry was derived from an equivalent circular patch. After calculating the effective radius r of the circular patch according to the standard formulation,

the circular boundary was approximated using six equal segments to form a regular hexagon. This methodology follows established practices for approximating polygonal patches from circular patches in high-frequency microstrip antenna design [21], preserving the effective radiating area and resonant characteristics while enhancing the uniformity of the surface current distribution. The effective radius of the equivalent circular patch is given by:

$$r = \frac{F}{\sqrt{\epsilon_{eff}}} \times \left[1 + \left(\frac{2 \times h}{(\pi \times F \times \epsilon_{eff})} \right) \times \left(\ln \left(\pi \times \frac{F}{2 \times h} \right) + 1.7726 \right) \right] \quad (1)$$

where $F = \frac{8.791 \times 10^9}{f_r}$, f_r represents the resonant frequency in Hz, h is the substrate height, and ϵ_{eff} is the effective dielectric constant. ϵ_{eff} is provided by:

$$\epsilon_{eff} = \frac{(\epsilon_r + 1)}{2} + \frac{(\epsilon_r - 1)}{2} \times \frac{1}{\sqrt{\left(1 + \frac{(12 \times h)}{W} \right)}} \quad (2)$$

where W is the microstrip line width, ϵ_r is the substrate relative permittivity, and h is the substrate thickness. Simulation results indicate that the proposed hexagonal antenna achieves excellent impedance matching at 28 GHz, with a minimum reflection coefficient of -40 dB, ensuring low return loss and efficient power transfer (Figure 2).

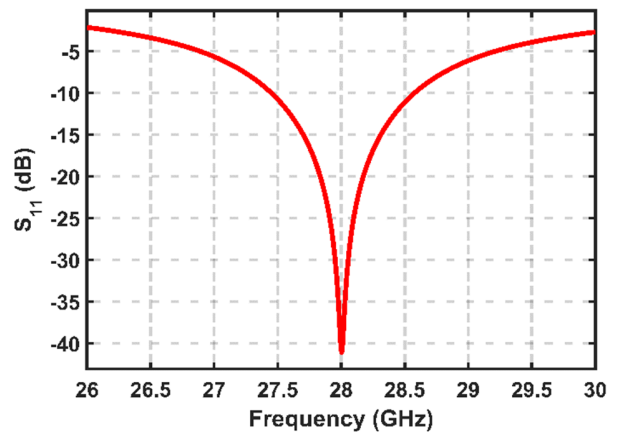


Fig. 2. Reflection coefficient (S_{11}) versus frequency for the proposed hexagonal antenna element.

The -10 dB impedance bandwidth is 1.12 GHz, corresponding to a fractional bandwidth of approximately 4%, and the Voltage Standing Wave Ratio (VSWR) is approximately unity at the resonance frequency, confirming proper impedance matching (Figure 3). The antenna provides a realized gain of 6.37 dB at 28 GHz (Figure 4). Antenna efficiency is evaluated in terms of radiation, as shown in Figure 5. At the resonance frequency, the single antenna element achieves a high efficiency of approximately 85%, indicating low radiation losses and effective power transfer. This high efficiency is primarily attributed to the good impedance matching and the optimized geometry of the radiating element, which ensure efficient radiation.

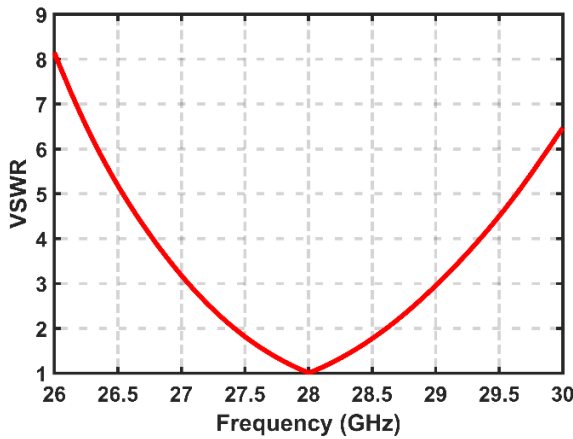


Fig. 3. VSWR versus frequency for the proposed hexagonal antenna element.

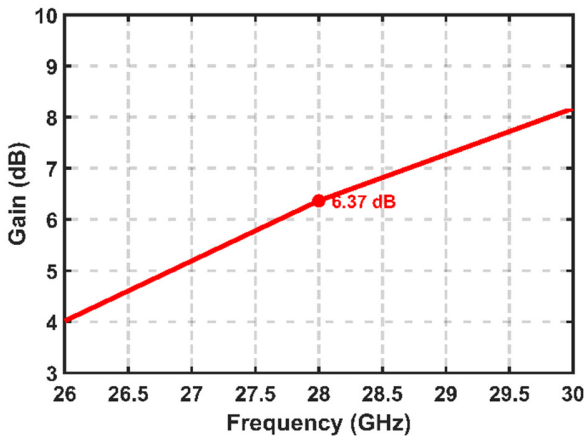


Fig. 4. Realized gain versus frequency of the hexagonal antenna element.

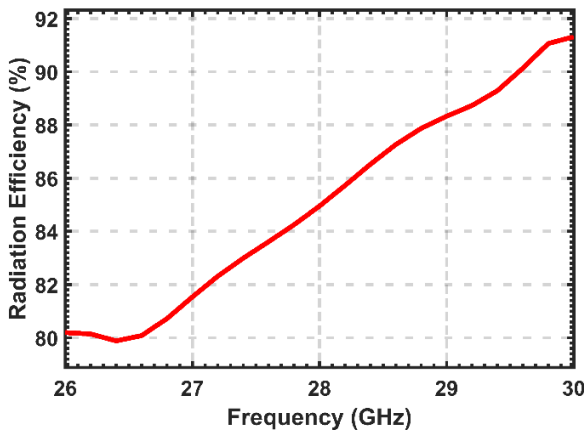


Fig. 5. Radiation efficiency of the proposed single antenna element.

The E-plane ($\phi = 0^\circ$) and H-plane ($\phi = 90^\circ$) radiation patterns are presented in Figures 6 and 7, with half-power beamwidths of 80.5° and 98.1° , respectively. Such performance demonstrates the suitability of the proposed antenna element for 28 GHz mmWave 5G applications, where stable directional radiation and controlled beamwidth are required.

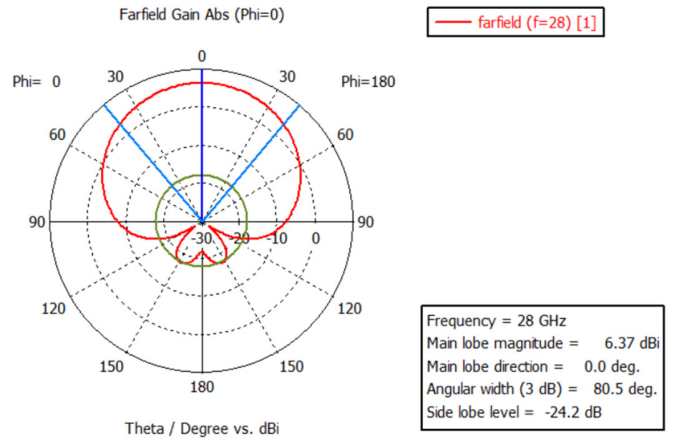


Fig. 6. E-plane ($\phi = 0^\circ$) radiation pattern of the hexagonal microstrip antenna element.

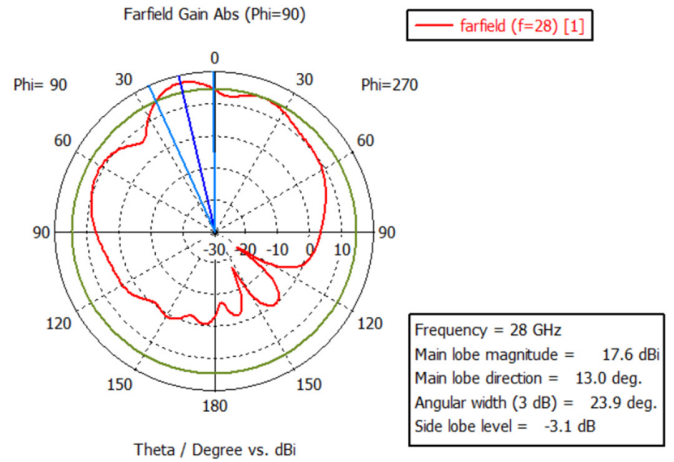


Fig. 7. H-plane ($\phi = 90^\circ$) radiation pattern of the hexagonal microstrip antenna element.

B. 1×8 Hexagonal Microstrip Antenna Array

The proposed 1×8 hexagonal microstrip antenna array, illustrated in Figure 8, significantly enhances the performance of the single-element antenna by increasing the number of radiating elements and exploiting array principles to achieve higher gain and directivity. The array is excited through a multi-stage corporate T-junction feeding network, which is fully modeled and optimized as a complete system in CST Microwave Studio. Starting from a single 50Ω input port, the feeding network progressively splits the input power through successive T-junctions until equal power is delivered to all eight radiating elements. At each junction, impedance matching is ensured using the parallel impedance formula:

$$Z_{in} = \left(\frac{1}{Z_1} + \frac{1}{Z_2} \right)^{-1}, \quad Z_1 = Z_2 = 2Z_{in} \quad (3)$$

where Z_{in} is the input impedance at the junction, and Z_1 and Z_2 are the impedances of the two branches. The corresponding microstrip line widths for each branch are calculated as:

$$w_{Z_i} = \left(\frac{377}{Z_i \sqrt{\epsilon_r}} - 2 \right) \times h \quad (4)$$

where w_{Z_i} is the microstrip line width for branch i , Z_i is the impedance of branch i ($i = 1, 2$), ϵ_r is the substrate relative permittivity, and h is the substrate thickness.

The optimized geometrical dimensions of the 1x8 hexagonal microstrip antenna array are summarized in Table II. The radiating elements are spaced by $d = 9.464 \text{ mm} \approx 0.88\lambda$ at 28 GHz, which reduces mutual coupling and avoids the occurrence of grating lobes.

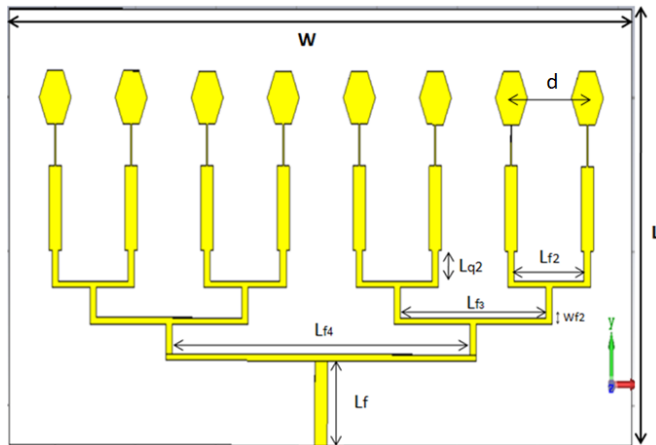


Fig. 8. Geometry of the 1x8 hexagonal antenna array.

TABLE II. OPTIMIZED GEOMETRICAL DIMENSIONS OF THE 1x8 HEXAGONAL MICROSTRIP ANTENNA ARRAY

Parameter	Value (mm)
Wa	1.58
Wq	0.15
Lq	2.7
Wf	1.55
Lf	4.5
Wq2	0.79
Lq2	1.98
Lf2	9.464
Wf2	0.4
Lf3	18.928
Lf4	37.856
W3	77.51
L3	27.90

Simulation results show that the proposed hexagonal antenna array exhibits good impedance matching at 28 GHz, with a minimum reflection coefficient of -28 dB (Figure 9). The -10 dB impedance bandwidth is 1.84 GHz, corresponding to a fractional bandwidth of 6.7%, and the VSWR is close to unity at the resonance frequency (Figure 10), confirming proper impedance matching and efficient power transfer. This behavior ensures uniform excitation and coherent radiation across the array elements.

The antenna array achieves a peak realized gain of 14.32 dB at 28 GHz (Figure 11). The radiation efficiency reaches approximately 89.5% at the resonance frequency (Figure 12), indicating low losses and effective bandwidth utilization.

The radiation patterns exhibit half-power beamwidths of 6.7° in the E-plane ($\phi = 0^\circ$) and 23.9° in the H-plane ($\phi = 90^\circ$), as shown in Figures 13 and 14. These results confirm that the proposed 1x8 hexagonal microstrip antenna array provides high gain, high efficiency, and well-controlled radiation characteristics for 28 GHz mmWave 5G applications.

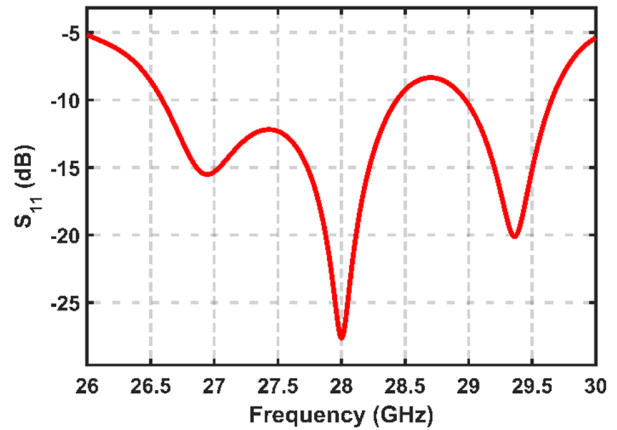


Fig. 9. Reflection coefficient (S_{11}) versus frequency of the 1x8 hexagonal antenna array.

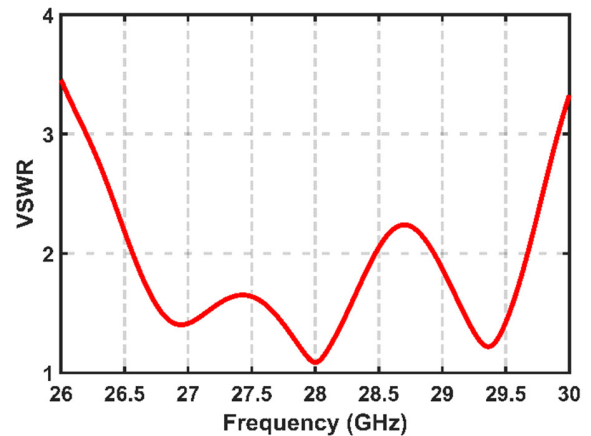


Fig. 10. VSWR versus frequency for the 1x8 hexagonal antenna array.

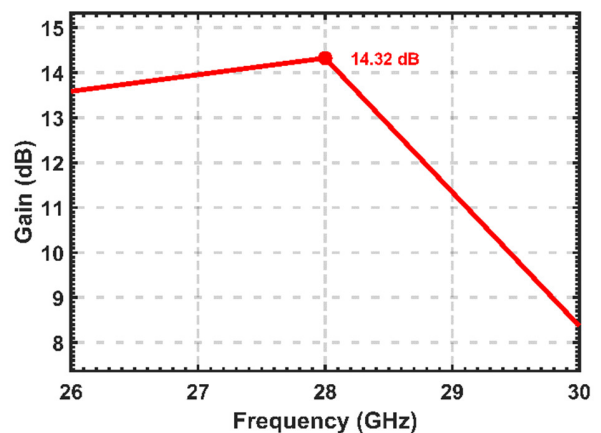


Fig. 11. Realized gain versus frequency for the 1x8 hexagonal antenna array.

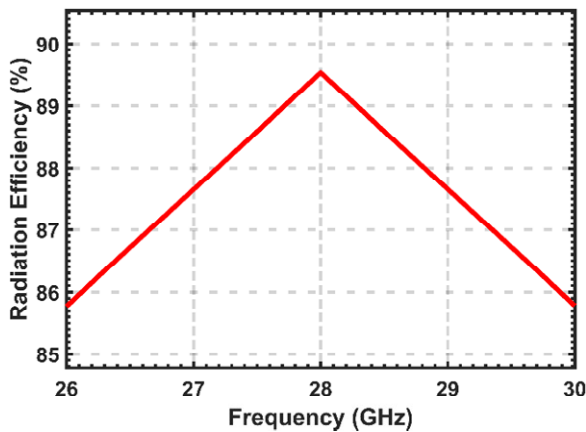


Fig. 12. Radiation efficiency of the proposed 1x8 antenna array.

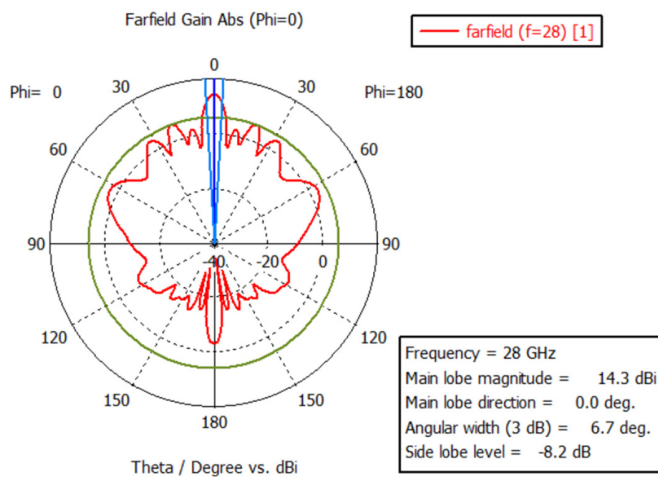


Fig. 13. E-plane ($\varphi = 0^\circ$) radiation pattern of the 1x8 hexagonal antenna array.

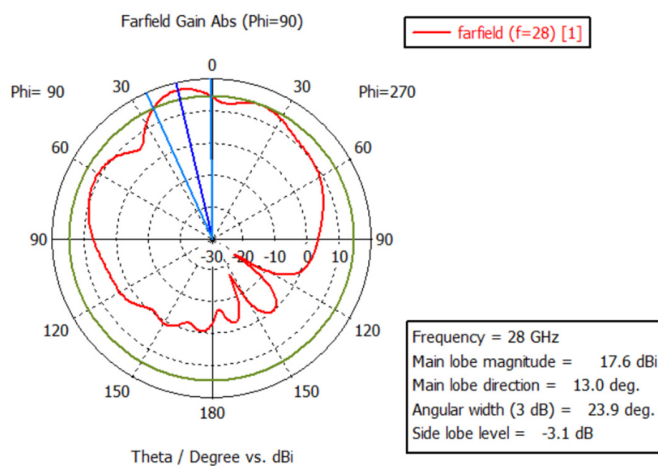


Fig. 14. H-plane ($\varphi = 90^\circ$) radiation pattern of the 1x8 hexagonal antenna array.

III. ANALYSIS AND DISCUSSION OF THE SIMULATION RESULTS

Full-wave electromagnetic simulations demonstrate that the single hexagonal patch antenna exhibits excellent impedance

matching at 28 GHz, with a minimum reflection coefficient of -33.93 dB and a -10 dB impedance bandwidth of 1.12 GHz, ensuring low return loss and efficient power transfer. The VSWR is approximately unity at the resonance frequency, and the antenna achieves a realized gain of 6.37 dB at 28 GHz, with half-power beamwidths of 80.5° and 98.1° in the E-plane ($\varphi = 0^\circ$) and H-plane ($\varphi = 90^\circ$), respectively. At the resonance frequency, the single antenna element attains a high radiation efficiency of approximately 85%, indicating low radiation losses and effective power transfer, which is primarily attributed to good impedance matching and the optimized geometry of the radiating element.

When implemented as a 1×8 hexagonal microstrip antenna array using a corporate T-junction feeding network, significant performance enhancements are observed, with the array achieving a peak realized gain of 14.32 dB at 28 GHz while maintaining excellent impedance matching, a VSWR close to unity, and an increased -10 dB impedance bandwidth of 1.84 GHz. Far-field analysis shows that for $\varphi = 0^\circ$, the main-lobe gain is 14.3 dB with a 3 dB beamwidth of 6.7° , whereas for $\varphi = 90^\circ$, the main-lobe gain reaches 17.6 dB with a 3 dB beamwidth of 23.9° . Moreover, the radiation efficiency of the proposed array remains high, with a peak value of approximately 89.5%, indicating low-loss operation and effective utilization of the radiating aperture.

These improvements in gain and bandwidth are attributed to the use of an antenna array, efficient aperture utilization enabled by the hexagonal geometry, coherent field superposition, optimized inter-element spacing greater than $\lambda/2$, and uniform power distribution with phase coherence ensured by the corporate T-junction feeding network, establishing the proposed hexagonal antenna array as a compact, efficient, and high-performance solution for 28 GHz mmWave 5G applications.

A. Comparison with Previous Works

Table III depicts a comparison between the antenna array and previously published arrays, including substrate, frequency, gain, and bandwidth. It appears that the proposed 1×8 array reaches higher gain and wider bandwidth than earlier array configurations, confirming its effectiveness for mmWave 5G applications

TABLE III. COMPARISON WITH PREVIOUS WORKS

Ref.	Resonance frequency (GHz)	Substrate material	Gain (dB)	Bandwidth (GHz)
[18]	28	RT5880	10.2	—
[17]	37	RT5880	12.8	0.677
[19]	28	RT5880	13.06	0.34
[22]	28	Rogers RO3003	6.6	1.23
[23]	28	Isola Gigaver 210	5.9	0.69
This work	28	RT5880	14.32	1.84

IV. CONCLUSION

This paper presented a novel 1×8 hexagonal microstrip antenna array operating at 28 GHz for fifth-generation (5G) millimeter-wave (mmWave) applications. The proposed array was numerically designed and analyzed on a Rogers RT5880 substrate and excited using a multi-stage corporate T-junction feeding network to ensure uniform power distribution among all radiating elements, enabling coherent radiation and consistent excitation.

Full-wave electromagnetic simulation results demonstrate that the antenna array achieves a high realized gain of approximately 14.32 dB, outperforming several previously reported microstrip-based arrays, along with a wide impedance bandwidth of 1.84 GHz, corresponding to a fractional bandwidth of 6.7%, which is suitable for mitigating severe propagation losses in mmWave communication environments. The hexagonal patch geometry enables efficient aperture utilization and improved surface current distribution. This results in a highly directive radiation pattern with a focused main lobe and reduced beamwidth, while maintaining a compact and planar structure that is well suited for practical integration into 5G mmWave systems. Future work will focus on extending the proposed design toward beamforming capabilities through the implementation of a Butler matrix.

REFERENCES

- [1] T. S. Rappaport *et al.*, "Wireless Communications and Applications Above 100 GHz: Opportunities and Challenges for 6G and Beyond," *IEEE Access*, vol. 7, pp. 78729–78757, 2019, <https://doi.org/10.1109/ACCESS.2019.2921522>.
- [2] T. S. Rappaport, Y. Xing, G. R. MacCartney, A. F. Molisch, E. Mellios, and J. Zhang, "Overview of Millimeter Wave Communications for Fifth-Generation (5G) Wireless Networks—With a Focus on Propagation Models," *IEEE Transactions on Antennas and Propagation*, vol. 65, no. 12, pp. 6213–6230, Dec. 2017, <https://doi.org/10.1109/TAP.2017.2734243>.
- [3] R. W. Heath, N. González-Prelcic, S. Rangan, W. Roh, and A. M. Sayeed, "An Overview of Signal Processing Techniques for Millimeter Wave MIMO Systems," *IEEE Journal of Selected Topics in Signal Processing*, vol. 10, no. 3, pp. 436–453, Apr. 2016, <https://doi.org/10.1109/JSTSP.2016.2523924>.
- [4] H. M. Marzouk, M. I. Ahmed, and A.-E. H. Shaalan, "Novel Dual-Band 28/38 GHz MIMO Antennas for 5G Mobile Applications," *Progress In Electromagnetics Research C*, vol. 93, pp. 103–117, June 2019, <https://doi.org/10.2528/PIERC19032303>.
- [5] R. N. Tiwari, D. Sharma, P. Singh, and P. Kumar, "A flexible dual-band 4 × 4 MIMO antenna for 5G mm-wave 28/38 GHz wearable applications," *Scientific Reports*, vol. 14, no. 1, June 2024, Art. no. 14324, <https://doi.org/10.1038/s41598-024-65023-2>.
- [6] P. S. B. Ghose *et al.*, "Dual-Band Antenna at 28 and 38 GHz Using Internal Stubs and Slot Perturbations," *Technologies*, vol. 12, no. 6, June 2024, Art. no. 84, <https://doi.org/10.3390/technologies12060084>.
- [7] K. Bharath, S. V. Nandigama, R. K. Dasari, and V. M. Pandharipande, "High Performance Millimeter Wave SIW Slotted Array Antenna," *Progress In Electromagnetics Research C*, vol. 125, pp. 15–23, Oct. 2022, <https://doi.org/10.2528/PIERC22072508>.
- [8] M. Edries, H. A. Mohamed, and A. A. Ibrahim, "A Dual Band 28/38 GHz Metamaterial Absorber for 5G Applications," *Journal of Infrared, Millimeter, and Terahertz Waves*, vol. 44, no. 11, pp. 898–911, Dec. 2023, <https://doi.org/10.1007/s10762-023-00948-9>.
- [9] W. A. Awan, M. Alibakhshikenari, and E. Limiti, "High Gain Dual Parasitic Patch Loaded Wideband Antenna for 28 GHz 5G Applications," in *2021 International Symposium on Antennas and Propagation*, Taipei, Taiwan, 2021, pp. 1–2, <https://doi.org/10.23919/ISAP47258.2021.9614441>.
- [10] P. Gupta, L. Malviya, and S. V. Charhate, "5G multi-element/port antenna design for wireless applications: a review," *International Journal of Microwave and Wireless Technologies*, vol. 11, no. 9, pp. 918–938, Nov. 2019, <https://doi.org/10.1017/S1759078719000382>.
- [11] T. Raj, R. Mishra, P. Kumar, and A. Kapoor, "Advances in MIMO Antenna Design for 5G: A Comprehensive Review," *Sensors*, vol. 23, no. 14, July 2023, Art. no. 6329, <https://doi.org/10.3390/s23146329>.
- [12] F. A. Almalki and M. C. Angelides, "An enhanced design of a 5G MIMO antenna for fixed wireless aerial access," *Cluster Computing*, vol. 25, no. 3, pp. 1591–1606, June 2022, <https://doi.org/10.1007/s10586-021-03318-z>.
- [13] M. B. E. Mashade and E. A. Hegazy, "Design and Analysis of 28GHz Rectangular Microstrip Patch Array Antenna," *WSEAS Transactions on Communications*, vol. 17, pp. 1–9, 2018.
- [14] A. Nayak, S. Dutta, and S. Mandal, "Design of Dual Band Microstrip Patch Antenna for 5G Communication Operating at 28 GHz and 46 GHz," *International Journal of Wireless and Microwave Technologies*, vol. 13, no. 2, pp. 43–52, Apr. 2023, <https://doi.org/10.5815/ijwmt.2023.02.05>.
- [15] J. Gao, K. Li, and H. Harada, "60 GHz wideband antenna with air filled stacked patch structure," in *2011 IEEE International Symposium on Antennas and Propagation*, Spokane, WA, USA, 2011, pp. 634–637, <https://doi.org/10.1109/APS.2011.5996791>.
- [16] M. Nahas, "A Super High Gain L-Slotted Microstrip Patch Antenna For 5G Mobile Systems Operating at 26 and 28 GHz," *Engineering, Technology & Applied Science Research*, vol. 12, no. 1, pp. 8053–8057, Feb. 2022, <https://doi.org/10.48084/etasr.4657>.
- [17] J. Khan, S. Ullah, U. Ali, F. A. Tahir, I. Peter, and L. Matekovits, "Design of a Millimeter-Wave MIMO Antenna Array for 5G Communication Terminals," *Sensors*, vol. 22, no. 7, Apr. 2022, Art. no. 2768, <https://doi.org/10.3390/s22072768>.
- [18] M. M. Kamal *et al.*, "Donut-Shaped mmWave Printed Antenna Array for 5G Technology," *Electronics*, vol. 10, no. 12, June 2021, Art. no. 1415, <https://doi.org/10.3390/electronics10121415>.
- [19] G. Mounir and J. E. Abbadi, "Antenna Array Design for 28 GHz Millimeter-Wave 5G Communication Systems," in *2024 7th International Conference on Advanced Communication Technologies and Networking*, Rabat, Morocco, 2024, pp. 1–4, <https://doi.org/10.1109/CommNet63022.2024.10793268>.
- [20] K. Benkhadda *et al.*, "1×2 microstrip patch antennas array for mm-waves 5G application," *TELKOMNIKA (Telecommunication Computing Electronics and Control)*, vol. 23, no. 1, pp. 40–47, Feb. 2025, <https://doi.org/10.12928/telkommika.v23i1.26263>.
- [21] C. A. Balanis, *Antenna Theory: Analysis and Design*, 3rd ed. Hoboken, NJ, USA: Wiley-Interscience, 2005.
- [22] A. E. Farahat and K. F. A. Hussein, "Dual-Band (28/38 GHz) Wideband MIMO Antenna for 5G Mobile Applications," *IEEE Access*, vol. 10, pp. 32213–32223, 2022, <https://doi.org/10.1109/ACCESS.2022.3160724>.
- [23] S.-E. Didi, I. Halkhams, M. Fattah, Y. Balboul, S. Mazer, and M. E. Bekkali, "Design of a 2×2 dual band 28/38 GHz MIMO antenna in millimeter band for 5G," *TELKOMNIKA (Telecommunication Computing Electronics and Control)*, vol. 22, no. 2, pp. 273–281, Apr. 2024, <https://doi.org/10.12928/telkommika.v22i2.25268>.